NEW ADAPTIVE METHOD FOR VOLTAGE SAG AND SWELL DETECTION

Mansour A. Mohamed

Electrical Engineering Department, Assiut University, Assiut 71518, EGYPT

Abstract   This paper presents an adaptive recursive least squares algorithm (ARLS) for detecting voltage sag and voltage swell events in power systems. Different methods have been developed to detect voltage sag and voltage swell. Some of them use window techniques, which are too slow when voltage sag or swell mitigation is required. Others depend on the extraction of a single non-stationary sinusoidal signal out of a given multi-components input signal, and therefore they don't consider the harmonic components in calculating the voltage root mean square value (rms). The method, proposed in this paper, is capable of estimating the voltage rms taking into account all harmonic components. The method is tested by applying it to different, simulated signals using ATP program, and compared with voltage sag detection algorithms.

• **Key Words :** Index Terms−Power quality monitoring, Adaptive algorithm, Harmonics, Voltage sag , Voltage swell.

1. Introduction

Due to dramatically increase of using nonlinear loads, such as power electronic equipment and sensitive computerized equipment as well as industrial drives, the issue of power quality (PQ) has gained renewed interest and become of great importance for the utilities and its customers. Such new loads are not only affected by service quality but also responsible for affecting adversely the quality of power supply. A large number of PQ disturbances have been reported in the literature. Some of them are transient in nature and others are periodic. Voltage sags and swells are widely recognized as one of the most important power quality aspects [1].

Voltage sags are defined as a decrease in the voltage root mean square (rms) value at power frequency for duration of *0.5* cycle to *1 min*[2]. Typical values of the voltage sags are between 10% and 90% of nominal voltage. The voltage swell limit is considered to be 110% of the nominal voltage value.Faults, large motor startup, transformer energizing and sudden load variations may cause voltage sag or swell. Voltage sags that may impact equipment are usually caused by faults on the power system [3]. A study submitted to Electric Power Research Institute (EPRI) entitled "The cost of power disturbances to industrial and digital economy companies," [4] shows that the U.S. economy is losing between $104 billion and $164 billion a year due to outages and another $15 billion to $24 billion due to PQ phenomena .

The first step towards mitigating the sag or swell problems is to detect the incident and the end time as well as the level of the voltage sags or swells. Robust, fast and accurate automated techniques for detection of voltage sags and swells are of primary importance before the implementation of mitigating methods to enhance the quality of the power

supplied. The advances in signal processing techniques and digital filters open up to new methodologies and approaches in automatic detection of voltage sags and swells. A number of automated algorithms have been published over the last decade. Monitoring a moving average window over at least half-cycle to calculate the rms value, with discrete Fourier transform (DFT) to return the magnitude and phase of each frequency component within the supply were developed [3], [5]. The drawback of these techniques is that the detection time may be delayed up to one cycle. Space vector control method [6] is used to detect sags in three-phase systems by converting the three-phase voltage into one phasor, which itself is comprised of two orthogonal components, but can not detect the swell one that occurs due to phase-to-phase fault in power systems.

Further contribution for quick detection of voltage sags and swells is based on extracting a single non-stationary sinusoidal signal out of a given multi-components input signal [7], [8] for estimating the amplitude, phase and frequency of the voltage sags. The rectified voltage algorithm [9]as an alternative algorithm is based on the comparison of the instantaneous rectified voltage with a reference-rectified voltage. The comparison is performed using an adjustable threshold value. The work presented in [10] is primarily based on the assumption of knowing the frequency components of the distorted voltage waveform and having the previous samples of the voltage signal for one cycle. The detection time of this method is varying from 10 ms to 20 ms. Thedisadvantage of this method is its latency to transient response of the detected signals along with its sensitivity to unknown harmonics.

Radial basis function (RBF) neural network [11] and improved S-transform [12] have proposed for characterizing and identifying different sag types.

In this paper an efficient and accurate adaptive recursive least squares algorithm (ARLS) is adapted to detect the voltage sags and the voltage swells. The voltage sag detection depends on the calculation of the true rms of the voltage signal. Application of the algorithm to different voltage sags and swells signals, showsthat the algorithm is fast, accurate, and practically applicable. In the next section three detection techniques of voltage sag and swell are summarized. In section III the adaptive recursive least squares algorithm is introduced. In section IV the simulation results of detecting voltage sags and swells are presented to verify the ability of the proposed detecting technique.

2. Voltage Sag and Swell Detection Methods

2.1 Voltage Peak Calculation

Voltage sag can be detected by calculating the peak value of the signal waveform. A two-sample technique, based on the assumption of having pure sinusoidal voltage waveform, is used for peak voltage estimation, by finding the maximum of the absolute value of the sampled signal over half cycle propagating window.

Let $v(n)$, and $v(n+1)$ be voltage samples measured at times $t(n)$, and $t(n+1)$ respectively, T_s be the sampling time interval, $\omega_o = 2\pi f o$ is the fundamental angular velocity , and V is the voltage signal peak amplitude. Then

$$v(n) = V \sin((n-1)\omega_o T_s). \tag{1}$$

The voltage sample $v(n+1)$ measured at the time interval $n+1$ is expressed in terms of the previous voltage samples as

$$v(n+1) = V \sin(n\omega_0 T_s)$$
$$= V \sin((n-1)\omega_o T_s)\cos(\omega_o T_s) + V \cos((n-1)\omega_o T_s)\sin(\omega_o T_s) \tag{2}$$

Substituting (1) into (2) and simplifying results in

$$V \cos((n-1)\omega_o T_s) = \frac{v(n+1) - v(n)\cos(\omega_o T_s)}{\sin(\omega_o T_s)}. \quad (3)$$

Adding the squares of (1) and (3) and then take the square root of the result, the corresponding equation for the signal peak is simply:

$$V = \sqrt{\frac{v^2(n) + v^2(n+1) - 2v(n)v(n+1)\cos(\omega_o T_s)}{(\sin(\omega_o T_s))^2}}. \quad (4)$$

The practicality of the two-sample technique is hindered by the fact that voltage signal in power system usually contaminated with harmonics. Therefore, this technique of detecting voltage sag and swell is not practically efficient.

2.2 Missing Voltage Technique

The missing voltage algorithm [10] is defined as the difference between a phase-locked loop (PLL) voltage waveform $v_{pll}(t)$ and the actual distorted voltage signal $v_{sag}(t)$. The phase-locked loop waveform will be locked in magnitude, frequency, and phase angle to the pre-sag voltage waveform. The missing voltage instantaneous value is

$$m(t) = v_{pll}(t) - v_{sag}(t), \quad (5)$$

where

$$v_{pll}(t) = A\sin(\omega t - \phi_a), \quad (6)$$

and

$$v_{sag}(t) = B\sin(\omega t - \phi_b). \quad (7)$$

Substituting (6) and (7) into (5) and simplifying, give:

$$m(t) = R\sin(\omega t - \psi), \quad (8)$$

where

$$R = \sqrt{A^2 + B^2 - 2AB\cos(\phi_b - \phi_a)},$$

and

$$\tan\psi = \frac{A\sin(\phi_a) - B\sin(\phi_b)}{A\cos(\phi_a) - B\cos(\phi_b)}.$$

2.3 Extraction of Non−Stationary Sinusoids

The dynamics of the algorithm are governed by a set of nonlinear differential equations, which represent the time-varying nature of the voltage signals. The amplitude, phase and frequency are considered functions of time. The voltage signal is expressed by [7]

$$v(t) = A(t)\sin(\omega(t)t + \varphi(t)) + \xi(t), \quad (9)$$

where A, ω, φ and ξ are the voltage time-varying amplitude, frequency, phase and the noise. The discretized equations of the algorithm can be written as

$$A(n+1) = A(n) + 2T_s\mu_1 e(n)\sin(\varphi(n)), \quad (10)$$

$$\omega(n+1) = \omega(n) + 2T_s\mu_2 e(n)A(n)\cos(\varphi(n)), \quad (11)$$

$$\varphi(n+1) = \varphi(n) + T_s\omega(n) + 2T_s\mu_2\mu_3 e(n)A(n)\cos(\varphi(n)), \quad (12)$$

$$\hat{v}(n) = A(n)\sin(\varphi(n)), \quad (13)$$

$$e(n) = v(n) - \hat{v}(n). \quad (14)$$

3. Adaptive Recursive Least Squares Algorithm

The voltage signal measured at the point of common coupling of a distribution system contains a significant power in the low order harmonics with varying amplitude depending on the load conditions and the degree of disturbances occur. The voltage signal digitized at the point of the measurement can be modeled as:

$$v(t) = \hat{v}(t) + \zeta(t) = V_o e^{-t/\tau} + \sum_{k=1}^{M} V_k \sin(k\omega t + \varphi_k) + \zeta(t)$$

$$= V_o e^{-t/\tau} + \sum_{k=1}^{M} V_{pk} \sin(k\omega t) + \sum_{k=1}^{M} V_{qk} \cos(k\omega t) + \zeta(t),$$

$$(15)$$

where M, ζ, V_k, φ_k, are the number of harmonics, noise, the magnitude and the phase angle of the kth harmonic, respectively.

$$V_{pk} = V_k \cos\varphi_k,$$

and

$$V_{qk} = V_k \sin\varphi_k.$$

Numerically, the signal in (15) can be written as:

$$v(n) = \hat{v}(n) + \zeta(t_n) = V_o e^{-t_n/\tau} + \sum_{k=1}^{M} V_{pk} \sin(k\omega t_n) + \sum_{k=1}^{M} V_{qk} \cos(k\omega t_n) + \zeta(t_n),$$

$$(16)$$

where n is the time index. Equation (16) can be written in matrix form as:

$$v(n) = W^T(n)X(n) + \zeta(n),\qquad (17)$$

where,

$$W(n) = \begin{bmatrix} W_o(n) \\ W_1(n) \\ W_k(n) \\ W_M(n) \\ W_{M+1}(n) \\ W_{M+k}(n) \\ W_{2M}(n) \end{bmatrix} = \begin{bmatrix} V_o(n) \\ V_{p1}(n) \\ V_{pk}(n) \\ V_{pM}(n) \\ V_{q1}(n) \\ V_{qk}(n) \\ V_{qM}(n) \end{bmatrix},\ \text{and}$$

$$X(n) = \begin{bmatrix} x_o(n) \\ x_1(n) \\ x_k(n) \\ x_M(n) \\ x_{M+1}(n) \\ x_{M+k}(n) \\ x_{2M}(n) \end{bmatrix} = \begin{bmatrix} e^{-(n-1)T_s/\tau} \\ \sin((n-1)\omega_o T_s) \\ \sin(k(n-1)\omega_o T_s) \\ \sin(M(n-1)\omega_o T_s) \\ \cos((n-1)\omega_o T_s) \\ \cos(k(n-1)\omega_o T_s) \\ \cos(M(n-1)\omega_o T_s) \end{bmatrix}.$$

The estimated linear output value of the voltage waveform at time $t_n = (n-1)T_s$ is given by

$$\hat{v}(n) = \mathbf{W}^T(n)\mathbf{X}(n) = \sum_{k=0}^{2M} W_k(n) x_k(n) \qquad (18)$$

The present error $\zeta(n)$ at the nth sample is defined to be the difference between the voltage measured sample $v(n)$ and the linear output value $\hat{v}(n)$. The weight vector is updated by using the adaptive RLS rule,

$$\mathbf{W}(n+1) = \mathbf{W}(n) + \mu\xi(n)\mathbf{X}(n),\qquad (19)$$

where μ is an acceleration factor . Therefore, the error is reduced by μ as the weight vector is changed. The structure of the recursive adaptive algorithm is $2M+1$ input vector and one linear output vector. It can be noticed that the input vector size is proportional with twice the number of harmonics contained in the voltage signal. The voltage signal is uniformly sampled with the sampling time $T_s = 1/f_s$. The weight vector $W(n)$ is $(2M+1)$ estimated at sample n.

4. Simulation Results

To test the performance of the proposed adaptive ARLS technique and to verify its ability of detecting voltage sags, different sags events are generated by parametric equations and ATP-EMTP simulation program [13]. The generated signals, using parametric equations, are sampled at 256 sample/cycle for power frequency of $50Hz$ with 10 cycles window. A three-phase distribution network is modeled to obtain different voltage sag signals. All voltage sags generated are due to faults. Four types of faults are simulated which are single-line-to ground fault (SLGF), line-to-line fault (LLF), double-line-

to-ground fault (DLGF), and three-phase-to-ground fault (3PGF). The fault type, location, and resistance are randomly selected as well as the initial time of the fault. For the sags with harmonics (according to the IEEE standard 519 [14]) the limits for individual voltage distortion is not to exceed *3%* and the total voltage distortion is not to exceed *5%*. The proposed algorithm is compared to the peak voltage method. To test the validity of the proposed method, mathematically modeled, with and without harmonic components, sag signals and ATP-EMTP generated signals are utilized.

4.1 Mathematically Modeled Signals

4.1.1 Sinusoidal Voltage Sag or Swell Signal

A sinusoidal voltage waveform of amplitude *311V* and power frequency of *50Hzis* used. The sag start time and threshold amplitude are *0.4013s* and *90%* of the nominal voltage, respectively. The sag amplitudes studied are between *0.1* and *0.85* per unit of the nominal voltage. Fig. 1 shows *50%* voltage sag signal and the proposed algorithm along with the peak algorithm for detecting the instant of sag inception. The adaptive RLS algorithm detects the sag at *0.405s*, while the peak algorithm detects it at *0.4164s*,. The sag ended at *0.8085s*, which detected by the adaptive RLS at *0.8122s*.

4.1.2 Harmonic Contaminated Voltage Sag or Swell Signal

To verify the validity of the ARLS algorithm for harmonic contaminated voltage sag signals, the signal modeled in (20) is used.

$$v(t) = V_1\sin(\omega_o t + \varphi_o) + V_5\sin(5\omega_o t + \varphi_5) + V_7\sin(7\omega_o t + \varphi_7)$$
$$+ V_{11}\sin(11\omega_o t + \varphi_{11}) + V_{13}\sin(13\omega_o t + \varphi_{13}). \quad (20)$$

The magnitude of the harmonics as a percentage of the fundamental component are *4%, 3%, 1%*, and *0.95* for the 5th, 7th, 11th, and 13th harmonic orders,

respectively. In Fig. 2, the adaptive RLS, and peak voltage algorithms are compared. The peak voltage technique is divided by $\sqrt{2}$ for the comparison purposes. As shown in Fig.2, the voltage is dropped to *70%* of its nominal value at *0.4013s*. The adaptive RLS algorithm detects the sag at *0.4045s*. Different sag amplitudes are used to compare the two methods. Results are shown in Table I. The voltage swell limit is considered to be 110% of the nominal voltage value. The voltage swellof variable amplitude between 110% and 150% are studied for both pure sinusoidal and distorted voltage signals. The amplitude of the harmonic components in the distorted swell signals is proportional to the limits indicated in the IEEE standard 519. Table II summarizes the results of swells detection.

4.2 EMTP−ATP Simulated Signals

EMTP-ATP program is used to model 24kV, 50Hz, three-phase simplified distribution network feeding three different loads through three lines of different lengths. The resistance and inductance of the system impedance are 0.711Ω, and 11.857 mH respectively. The lengths of line 1, 2, and 3 are 8 km, 13 km, 20 km respectively. The per phase resistance, inductance, and capacitance of the lines are 0.1064 Ω/m, 0.0397mH/m, and 0.00029μF/m respectively.Fig. 3 shows a single line diagram of the simplified distribution network. Line (1) is the shortest line in the studied test system; therefore, fault location is chosen to be at the receiving end of line (1). All voltage sags modeled are due to faults at the terminalsof load1. Four types of faults are simulated: single-line-to ground fault (SLGF), line-to-line fault (LLF), double-line-to-ground fault (DLGF), and three-phase-to-ground fault (3PGF). The fault resistance is taken to be zero (bolted fault).

A snapshot of three-phase voltages measured at the point of common coupling (PCC) due to DLGF at the terminal of load1 is shown in Fig. 4. The instant of fault occurrence is at 0.6052 s. The fault cleared at

0.8052s. Phase A and B inhabited voltage sags of about 20%. On the other hand, phase C inhabited voltage swell more than 150%. Figs. 5-6illustrate the capability of the adaptive RLS to detect sags in real time and show a comparison of the adaptive RLS against the Peak voltage detecting a sag in real time. Fig. 7 shows a comparison of the adaptive RLS against the Peak voltage detecting the occurrence of swell on phase C.

It is seen from the figures, that the proposed algorithm is able to detect the voltage sag and swell fasterthan the peak method.

[Fig. 2] Detection of voltage sag in distorted voltage signal.

[Fig. 1] Detection of 50% voltage sag by peak voltage and adaptive RLS.

[Fig. 3] Test system

[Table I] Detection of Sag Inception and End with and without harmonics and different sag amplitudes using RLS and Peak amplitude techniques

Sag amplitude	0.1	0.2	0.3	0.4	0.5	0.6	0.7	0.8	0.85
Event	Voltage sag incepted at 0.4013 s								
RLS	0.4034	0.4035	0.403	0.4035	0.4039	0.4043	0.4050	0.4042	0.4033
Peak	0.4165	0.4165	0.4165	0.4165	0.4163	0.4165	0.4164	0.4165	0.4168
Event	Voltage sag ended at 0.8 s								
RLS	0.8040	0.8041	0.8036	0.8040	0.8036	0.8045	0.8032	0.8030	0.8022
Peak	0.8136	0.8136	0.8136	0.8136	0.8136	0.8136	0.8168	0.8137	0.8132
Event	Voltage sag with harmonics incepted at 0.4013 s								
RLS	0.4036	0.4035	0.4037	0.4038	0.4041	0.4045	0.4054	0.4128	0.4143
Peak	0.4165	0.4165	0.4165	0.4170	0.4163	0.4165	0.4165	0.4165	0.4165
Event	Voltage sag with harmonics ended at 0.8 s								
RLS	0.8136	0.8138	0.8139	0.8139	0.8139	0.8137	0.8131	0.8062	0.8042
Peak	0.8135	0.8135	0.8153	0.8135	0.8135	0.8135	0.8135	0.8135	0.8135

[Table II] Detection of Swells Inception and End with and without harmonics and different swell amplitudes using RLS and Peak amplitude techniques

| Swell amplitude	1.15	1.2	1.3	1.4	1.5
Event	Voltage swells incepted at 0.4013 s				
RLS	0.4086	0.4061	0.4041	0.4034	0.4023
Peak	0.4143	0.4136	0.40128	0.4127	0.4126
Event	Voltage swells ended at 0.8 s				
RLS	0.8045	0.8053	0.8071	0.8077	0.8074
Peak	0.8160	0.8165	0.8169	0.8171	0.8175
Event	Voltage swells with harmonics incepted at 0.4013 s				
RLS	0.4074	0.4065	0.4041	0.4034	0.4027
Peak	0.4139	0.4135	0.4132	0.4129	0.4128
Event	Voltage swells with harmonics ended at 0.8 s				
RLS	0.8030	0.8042	0.8065	0.8078	0.8081
Peak	0.8165	0.8164	0.8167	0.8169	0.8172
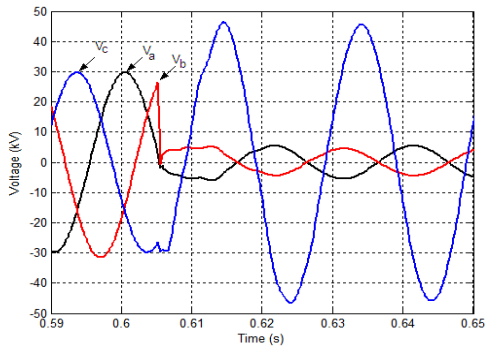
[Fig. 4] Three-phase voltages measured at PCC due to DLGF at load1.
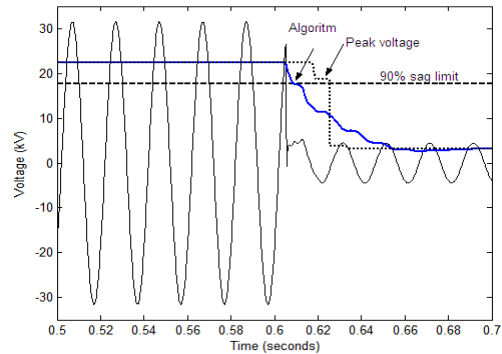
[Fig. 6] Phase B voltage sag detected by the adaptive RLS and by peak voltage algorithms.
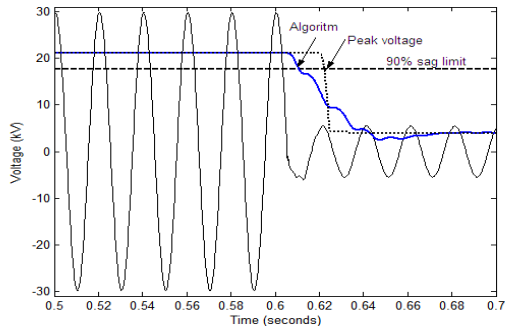
[Fig. 5] Phase A voltage sag detected by the adaptive RLS and by peak voltage algorithms.
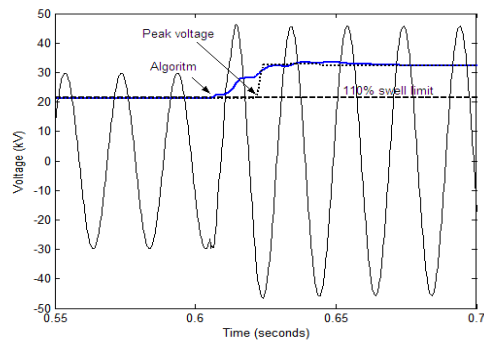
[Fig. 7] Phase C voltage swell detected by the adaptive RLS and by peak voltage algorithms.

5. Conclusions

An adaptive recursive least squares algorithm has been developed for voltage sag and swell detection in power systems. Voltage sag and swell detection, using this method, depends on the calculation of the true rms value of the voltage signals, which makes it more accurate. Voltage sag and swell signals, with different amplitudes have been investigated. The method has been compared with the peak voltage sag detection method. Results show that the method is faster than the Peak technique. The simplicity of the technique calculations with no prior knowledge requirements make it feasible for being practically applicable.

REFERENCES

[1] M. F. McGranaghan, D. R. Ruller, and M. J. Samotyi, "Voltage sags in industrial power systems," IEEE Trans. on Industry Applications, Vol. 29, No. 2, pp. 379-403, 1993.

[2] IEEE Recommended Practice for Monitoring Electric Power Quality, 1995. ANSI/IEEE standard 1159.

[3] P. Wang, N. Jenkins, and M. H. J. Bollen, "Experimental investigation of voltage sag mitigation by an advanced static VAR compensator," IEEE Trans. Power Delivery, Vol. 13, No. 4, pp. 1641-1647, 1998.

[4] EPRI CEIDS Report, "The cost of power disturbances to industrial and digital economy companies," Executive Summary, 2001.

[5] W. Lee, B. Han, and H. Cha, "Three-phase dynamic voltage restorer with a robust voltage sag detection method," in Proc. 2nd IEEE ENERGYCON conference and exhibition, pp. 533-538, 2012.

[6] C. Zhan, V. K. Ramachandaramurthy, A. Arulampalam, C. Fitzer, S. kromlidis, M. Barnes, and N. Jenkins, "Dynamic voltage restorer based on voltage space vector PWM control," IEEE Trans. Industry Applications, Vol. 37, pp. 1855-1863, 2001.

[7] R. Naidoo, and P. Pillay, "A new method of voltage sag and swell detection," IEEE Trans. Power Delivery, Vol. 22, No. 2, pp. 1056-1063, 2007.

[8] S. Kamble, and C. Thorat, "A new algorithm for voltage sag detection," in Proc. IEEE Int. Conf. Advances in Engineering, Science and Management, ICAESM 2012, pp. 138-143, 2012.

[9] Florio, and M. Mazzucchelli, "Voltage sag detection based on rectified voltage processing," IEEE Trans. Power Delivery, Vol. 19, No. 4, pp. 1962-1967, 2004.

[10] Fitzer, M. Barnes, and P. Green, "Voltage sag detection technique for a dynamic voltage restorer," IEEE Trans. Industry Applications, Vol. 40, No. 14, pp. 203-212, 2004.

[11] G. Lu, and X. Wang, "Voltage sag detection and identification based on phase-shift and RBF neural network," in Proc. 4th Int. Conf. Fuzzy Systems and Knowledge Discovery, pp. 684-688, 2007.

[12] M. Khosravi, M. A. Hajibagherifard, and M. T. Bina, "The study of voltage sag detection by improved S-transform," in Proc. 3rd Power Electronics and Drive systems Technology (PEDSTC) Conference, pp. 160-163, 2012,

[13] H. W. Dommel, Electromagnetic Transients Program. Reference Manual (EMTP Theory Book), Bonneville Power Administration, Portland, 1986.

[14] IEEE Recommended Practices and Requirements for Harmonics Control in Power Systems (ANSI), IEEE 519 std., 1992.

저자소개

Mansour A. Mohamed

· 1990 : Assiut University, Assiut,
  Egypt (BEng)
· 1996 : Assiut University, Assiut,
  Egypt (Msc(Eng))
· 2003 : Eng. from Arizona State
  University, United states (Ph.D)
· E-Mail : mamohamed2004@yahoo.com
<Research Interest> : Power Quality, Power
  Transmission and distribution analysis